

# Role of beam propagation in Goos–Hänchen and Imbert–Fedorov shifts

A. Aiello\* and J. P. Woerdman

Huygens Laboratory, Leiden University, P.O. Box 9504, 2300 RA Leiden, The Netherlands

\*Corresponding author: aiello@molphys.leidenuniv.nl

Received April 22, 2008; revised May 26, 2008; accepted May 26, 2008;  
posted May 29, 2008 (Doc. ID 94942); published June 23, 2008

We derive the polarization-dependent displacements parallel and perpendicular to the plane of incidence for a Gaussian light beam reflected from a planar interface, taking into account the propagation of the beam. Using a classical-optics formalism we show that beam propagation may greatly affect both Goos–Hänchen and Imbert–Fedorov shifts when the incident beam is focused. © 2008 Optical Society of America  
OCIS codes: 240.3695, 260.5430.

It is known that the behavior of bounded beams of light reflected from and transmitted through a planar interface differs from that exhibited by plane waves, the latter being ruled by Snell's law and the Fresnel equations [1]. For bounded beams diffractive corrections occur, the most prominent of which are the so-called Goos–Hänchen (GH) [2] and Imbert–Fedorov (IF) shifts [3] of the beam, occurring in the directions parallel and perpendicular to the plane of incidence, respectively. In principle, both reflected and transmitted beams are subject to such shifts. A great deal of literature exists about experimental [4,5] and theoretical [6–9] demonstrations of both GH and IF shifts but generally the effects of beam propagation are not accounted for [10]. A notable exception is a recent paper by Hosten and Kwiat [11] where the authors report, among other issues, on a dramatic signal enhancement technique ( $\sim 100\times$ ) for a *quantum* version of the IF shift, the spin Hall effect of light (SHEL), based on beam propagation [12]. The theoretical discussion in [11] uses the quantum formalism of weak measurements [13], although the authors note that the *beam propagation enhancement* (BPE) is essentially a classical phenomenon.

The purpose of this Letter is to present a purely classical analysis of the BPE; we feel that this is useful since a classical description will make this important technique, which allows subnanometer sensitivity [11], more accessible to the metrology community. Furthermore, our classical framework covers both the GH and the IF cases, whereas the treatment in [11] is restricted to the IF case only. A last, minor, difference between the present work and that of Hosten and Kwiat [11] is that the latter authors measure the beam that is transmitted across an air–glass interface, while we study the beam that is reflected by such an interface. Since the transmission and reflection cases have a very similar mathematical structure, all our main conclusions regarding reflective GH and IF shifts remain qualitatively valid for the transmission case.

We begin by considering optical reflection from a planar interface; Fig. 1 illustrates the coordinate system. The  $z$  axis of the laboratory Cartesian frame ( $xyz$ ) is normal to the planar interface ( $z=0$ ), that separates empty space (in practice air), where  $z < 0$ ,

from an optically dense region (either a dielectric or a metal [14]), where  $z > 0$ . We use a Cartesian frame ( $x_i, y_i, z_i$ ) attached to the incident beam and another one ( $x_r, y_r, z_r$ ) attached to the reflected beam. Note that the coordinate  $x_r$  is associated with the longitudinal GH shift, while  $y_r$  is associated with the transverse IF shift. Consider a monochromatic Gaussian beam of light propagating in air parallel to the positive  $z_i$  axis. The electric field amplitude of such a beam can be written as [9]

$$\mathbf{E}^{\text{inc}} \propto \exp \left[ iZ_i - \frac{X_i^2 + Y_i^2}{2(\Lambda + iZ_i)} \right] \times \left( \hat{\mathbf{x}}_i f_P + \hat{\mathbf{y}}_i f_S - i\hat{\mathbf{z}}_i \frac{f_P X_i + f_S Y_i}{\Lambda + iZ_i} \right), \quad (1)$$

where we have introduced the dimensionless variables  $X_i = kx_i$ ,  $Y_i = ky_i$ ,  $Z_i = kz_i$ ,  $\Lambda = kL$ , and where the paraxial approximation corrected up to first-order derivatives has been used [15]. The Gaussian amplitude of the beam is characterized by the minimum waist  $w_0$  located at  $z_i=0$  and the Rayleigh range  $L = kw_0^2/2$ . The polarization of the beam is determined by the complex-valued unit vector  $\hat{\mathbf{f}} = (f_P \hat{\mathbf{x}}_i + f_S \hat{\mathbf{y}}_i) / (|f_P|^2 + |f_S|^2)^{1/2}$ , which corresponds experimentally to a polarizer perpendicular to the beam central

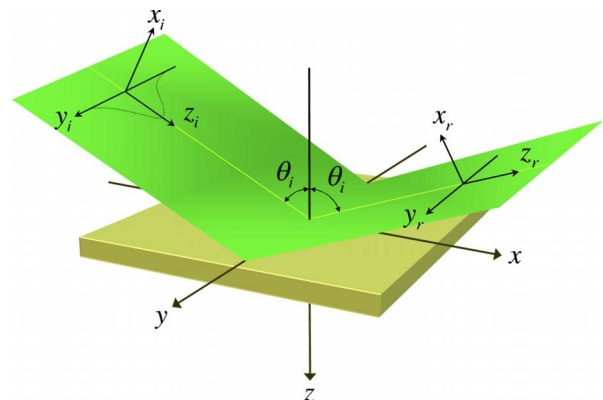


Fig. 1. (Color online) Geometry of beam reflection at the air–medium interface.

wave vector  $\mathbf{k}_i = k\hat{\mathbf{z}}_i$ . Across the interface  $z=0$  the tangential components of the electric and magnetic field must be continuous. From this boundary condition and Eq. (1) the electric and magnetic fields of the reflected beam can be determined under the same conditions. A straightforward calculation [9] yields

$$\begin{aligned} \mathbf{E}^{\text{ref}} \propto \exp \left[ iZ_r - \frac{X_r^2 + Y_r^2}{2(\Lambda + iZ_r)} \right] \\ \times \left\{ \hat{\mathbf{x}}_r \left[ f_P r_P \left( 1 - i \frac{X_r}{\Lambda + iZ_r} \frac{\partial \ln r_P}{\partial \theta_i} \right) \right. \right. \\ \left. \left. + if_S \frac{Y_r}{\Lambda + iZ_r} (r_P + r_S) \cot \theta_i \right] \right. \\ \left. + \hat{\mathbf{y}}_r \left[ f_S r_S \left( 1 - i \frac{X_r}{\Lambda + iZ_r} \frac{\partial \ln r_S}{\partial \theta_i} \right) \right. \right. \\ \left. \left. - if_P \frac{Y_r}{\Lambda + iZ_r} (r_P + r_S) \cot \theta_i \right] \right. \\ \left. - i\hat{\mathbf{z}}_r \left( \frac{r_P f_P X_r + r_S f_S Y_r}{\Lambda + iZ_r} \right) \right\}, \end{aligned} \quad (2)$$

where  $X_r = kx_r$ ,  $Y_r = ky_r$ ,  $Z_r = kz_r$ , and  $r_A, \partial r_A / \partial \theta_i$  are the Fresnel reflection coefficients and their first derivatives evaluated at the “central” angle of incidence  $\theta_i = \arccos(\mathbf{k}_i \cdot \hat{\mathbf{z}}/k)$ , respectively. The index  $A \in \{P, S\}$  is a label for a linearly polarized plane wave whose electric field vector is either parallel ( $P$ ) or perpendicular ( $S$ ) to the plane of incidence ( $x, z$ ), which is defined as the common plane of the central wave vector  $\mathbf{k}_i = k\hat{\mathbf{z}}_i$ , and the normal to the interface  $\hat{\mathbf{z}}$ . In a similar manner the magnetic field  $\mathbf{B}^{\text{ref}}$  of the reflected beam can be obtained and used to calculate the beam intensity spatial profile  $I(X_r, Y_r, Z_r)$  as the flux of the time averaged Poynting vector  $\bar{\mathbf{S}} \propto \text{Re}(\mathbf{E}^{\text{ref}} \times \mathbf{B}^{\text{ref}*})$  through a surface perpendicular to the central direction of propagation  $\hat{\mathbf{z}}_r$ :  $I(X_r, Y_r, Z_r) \propto \bar{\mathbf{S}} \cdot \hat{\mathbf{z}}_r$ . At any given plane  $Z_r = \text{const.}$ , the intensity  $I(X_r, Y_r, Z_r)$  can be considered as the distribution of the “quasi-Gaussian” variables  $\mathbf{X} = X_r \hat{\mathbf{x}}_r + Y_r \hat{\mathbf{y}}_r$  with means  $\mathbf{M} = \langle X_r \rangle \hat{\mathbf{x}}_r + \langle Y_r \rangle \hat{\mathbf{y}}_r$ , where

$$\mathbf{M} = \frac{\int \int \mathbf{X} I(X_r, Y_r, Z_r) dX_r dY_r}{\int \int I(X_r, Y_r, Z_r) dX_r dY_r}, \quad (3)$$

determines the centroid of the reflected beam [16]. As the result of a straightforward calculation one obtains for the GH shift

$$\langle X_r \rangle = \frac{\varphi_P R_P^2 a_P^2 + \varphi_S R_S^2 a_S^2}{R_P^2 a_P^2 + R_S^2 a_S^2} - \frac{Z_r}{\Lambda} \frac{\rho_P R_P^2 a_P^2 + \rho_S R_S^2 a_S^2}{R_P^2 a_P^2 + R_S^2 a_S^2}, \quad (4)$$

and for the IF shift

$$\begin{aligned} \langle Y_r \rangle = - \frac{a_P a_S \cot \theta_i}{R_P^2 a_P^2 + R_S^2 a_S^2} \left\{ [(R_P^2 + R_S^2) \right. \\ \times \sin \eta + 2R_P R_S \sin(\eta - \phi_P + \phi_S)] \\ \left. - \frac{Z_r}{\Lambda} (R_P^2 - R_S^2) \cos \eta \right\}, \end{aligned} \quad (5)$$

where  $r_A \equiv R_A \exp(i\phi_A)$ ,  $A \in \{P, S\}$ ,  $f_P = a_P \in \mathbb{R}$ ,  $f_S = a_S \exp(i\eta)$ , and  $\rho_A = \text{Re}(\partial \ln r_A / \partial \theta_i)$ ,  $\varphi_A = \text{Im}(\partial \ln r_A / \partial \theta_i)$ .

Equations (4) and (5) are the first main result of this Letter. They give both the GH and the IF shift as functions of the beam propagation distance  $Z_r$ . For a well-collimated beam, the condition  $Z_r/\Lambda \ll 1$  is trivially satisfied at optical frequencies and the  $Z_r$ -independent terms in both Eqs. (4) and (5) are dominant. Such terms represent the “traditional” GH and IF shifts. In fact, when  $Z_r=0$  Eq. (4) is a straightforward generalization of the well-known Artmann formula [17]; Eq. (5) is in agreement with Bliokh and Bliokh [18]. However, for a focused beam the condition  $Z_r/\Lambda \gg 1$  may hold and the  $Z_r$ -dependent terms become relevant. For example, if a typical He–Ne laser operating at wavelength  $\lambda$  of 633 nm with a minimum waist  $w_1$  of 1.5 mm is focused by a lens with a focal length  $f$  of 100 mm, a waist of  $w_0 = \lambda f / (\pi w_1) \approx 13 \mu\text{m}$  is produced. If this beam propagates over a distance of 250 mm from the lens, we easily obtain  $Z_r/\Lambda \approx 168$  [19]. Thus, depending on the actual experimental conditions, either  $Z_r$ -dependent or -independent terms in Eqs. (4) and (5) may be dominant and, as a consequence, the measured GH and IF shifts will change dramatically.

To show the connections between the results above and the ones presented in [11], we must take a step backward and calculate, as an illustrative example, the quantity  $\hat{\mathbf{x}}_r \cdot \mathbf{E}^{\text{ref}}$  evaluated for  $a_S = 0$  on the plane of incidence  $Y_r = 0$ . This corresponds to an experimental configuration apt to measure the GH shift of a  $P$ -polarized beam. From Eq. (2) it readily follows that

$$\begin{aligned} \hat{\mathbf{x}}_r \cdot \mathbf{E}^{\text{ref}} \propto \exp \left[ - \frac{X_r^2}{2(\Lambda + iZ_r)} \right] \left( 1 - i \frac{X_r}{\Lambda + iZ_r} \frac{\partial \ln r_P}{\partial \theta_i} \right) \\ \sim \exp \left[ - \frac{(X_r - \varphi_P + i\rho_P)^2}{2(\Lambda + iZ_r)} \right]. \end{aligned} \quad (6)$$

A careful inspection of the equation above shows that it represents a Gaussian beam tilted clockwise by an angle  $\rho_P/\Lambda$  with respect to the axis  $\hat{\mathbf{z}}_r$  and displaced by  $\varphi_P/k$  along the axis  $\hat{\mathbf{x}}_r$ . In other words, for a Gaussian beam an *imaginary* position shift is equivalent to an angular tilt, while a *real* one represents a spatial shift. It is easy to see that the complex-valued nature of the shift controls its behavior under beam propagation. To demonstrate this we note that calculation of the centroid of the distribution  $|\hat{\mathbf{x}}_r \cdot \mathbf{E}^{\text{ref}}|^2$  yields

$$\langle X_r \rangle = \varphi_P - (Z_r/\Lambda)\rho_P, \quad (7)$$

which coincides with Eq. (4) evaluated for  $\alpha_S=0$ . This expression of  $\langle X_r \rangle$  shows that only the imaginary part  $\rho_P$  of the complex shift  $\varphi_P - i\rho_P$  couples to the coordinate  $Z_r$ , and it is enhanced by a factor  $Z_r/\Lambda$  as the reflected beam propagates along the optical distance  $Z_r$ . As will be shown below, such a factor  $Z_r/\Lambda$  coincides with the propagation enhancement factor  $F$  of [11], which lies at the core of their signal enhancement technique. Although in the reasoning above we have considered a specific example, it is not difficult to realize that the conclusions reached are perfectly general; in particular, positioning of the waist of the Gaussian beam at the interface is not essential (see also [11]). This is the second main result of our Letter.

We conclude this Letter by demonstrating that, as anticipated, the term  $Z_r/\Lambda$  in our Eq. (7) coincides with the propagation enhancement factor  $F$  of Hosten and Kwiat [11]. According to their scheme the incident beam is first preselected in the  $P$  polarization state—namely,  $f_P=1$ ,  $f_S=0$ —and then postselected (after reflection by an air–glass interface) in the  $\hat{\nu}$  polarization state, where  $\hat{\nu} = \hat{x}_r \sin \Delta + \hat{y}_r \cos \Delta$  and  $\Delta = \pm|\Delta|$ . In addition, after reflection the beam is observed along the transverse plane  $X_r=0$ . Thus, the relevant amplitude of the reflected field can be written as

$$\begin{aligned} \hat{\nu} \cdot \mathbf{E}^{\text{ref}}|_{X_r=0} &\propto \exp\left[-\frac{Y_r^2}{2(\Lambda + iZ_r)}\right] \left(1 + i\frac{Y_r D \cot \Delta}{\Lambda + iZ_r}\right) \\ &\sim \exp\left[-\frac{(Y_r - iD \cot \Delta)^2}{2(\Lambda + iZ_r)}\right], \end{aligned} \quad (8)$$

where the purely imaginary term  $iD \cot \Delta$  is described in [11] as the product of the SHEL-induced photon displacement  $D=(1+r_S/r_P)\cot \theta_i$  and the weak value of the photon spin component  $i \cot \Delta$ . However, by comparing Eq. (8) with Eq. (6) it is clear that at a classical level such an imaginary shift amounts to a tilt by the small angle  $D \cot \Delta/\Lambda$  of the reflected beam. From the discussion above we know that an imaginary shift couples with coordinate  $Z_r$ , and, therefore, increases as the beam propagates. In fact, calculation of the centroid of the distribution  $|\hat{\nu} \cdot \mathbf{E}^{\text{ref}}|_{X_r=0}|^2$  yields

$$\langle Y_r \rangle = (Z_r/\Lambda)D \cot \Delta, \quad \langle Y_r^2 \rangle = (\Lambda^2 + Z_r^2)/(2\Lambda), \quad (9)$$

where  $Z_r/\Lambda \equiv F$  ( $\approx 156$  in [11]) is just the propagation enhancement factor. This last equality can be easily proved by combining the two formulas in Eq. (9) to obtain, in terms of dimensional variables,

$$\langle y_r \rangle = \frac{2k\langle y_r^2 \rangle}{R(z)} \delta \cot \Delta \approx \frac{4\pi\langle y_r^2 \rangle}{z\lambda} \delta \cot \Delta, \quad (10)$$

where  $\delta=D/k$ ;  $R(z)=(z^2+L^2)/z \approx z$  is the radius of curvature of the beam wavefront at the lens L2 position [20]; and the last approximate equality holds in the experimental conditions of [11], where  $z/L \gg 1$ .

From Eq. (10) it readily follows that  $F=4\pi\langle y_r^2 \rangle/(z\lambda)$ , in agreement with Eq. (4) in [11].

In summary, we have furnished analytic expressions, based upon classical optics, for both the GH and the IF shifts, as functions of the beam propagation distance. These give in a natural way the dramatic changes of the GH and IF displacements induced by using a focused beam. Moreover, from the analysis of such expressions we derived a fully classical interpretation of a very recently introduced signal enhancement technique employed to measure the spin Hall effect of light [11].

We acknowledge Michele Merano for useful discussions. This project is supported by FOM.

## References and Notes

1. M. Born and E. Wolf, *Principles of Optics*, 7th ed. (Cambridge U. Press, 2003).
2. F. Goos and H. Hanchen, *Ann. Phys.* **1**, 333 (1947).
3. O. Costa de Beauregard and C. Imbert, *Phys. Rev. Lett.* **28**, 1211 (1972).
4. C. Imbert, *Phys. Rev. D* **5**, 787 (1972).
5. F. Pillon, H. Gilles, and S. Girard, *Appl. Opt.* **43**, 1863 (2004).
6. W. Nasalski, *Phys. Rev. E* **74**, 056613 (2006).
7. K. Yu. Bliokh and Yu. P. Bliokh, *Phys. Rev. Lett.* **96**, 073903 (2006).
8. H. M. Lai, C. W. Kwok, Y. W. Loo, and B. Y. Xu, *Phys. Rev. E* **62**, 7330 (2000).
9. A. Aiello and J. P. Woerdman, arXiv:0710.1643v2 [physics.optics] (2007).
10. The literature on these topics is so vast that it is impossible to cite the complete bibliography. As an example, see [4–8] and references therein.
11. O. Hosten and P. Kwiat, *Science* **319**, 787 (2008).
12. It should be noted, however, that in [11] an additional signal enhancement technique based upon polarization control is employed. In this Letter we do not cover such issues since for Gaussian beams the propagation factor is independent of polarization.
13. Y. Aharonov, D. Z. Albert, and L. Vaidman, *Phys. Rev. Lett.* **60**, 1351 (1988).
14. M. Merano, A. Aiello, G. W. 't Hooft, M. P. van Exter, E. R. Eliel, and J. P. Woerdman, *Opt. Express* **15**, 15928 (2007).
15. H. A. Haus and J. L. Pan, *Am. J. Phys.* **61**, 818 (1993).
16. C.-F. Li, *Phys. Rev. A* **76**, 013811 (2007).
17. K. Artmann, *Ann. Phys.* **437**, 87 (1948).
18. K. Yu. Bliokh and Yu. P. Bliokh, *Phys. Rev. E* **75**, 066609 (2007).
19. It should be noted for these “experimental” data the angular aperture  $\vartheta=\lambda/(2\pi w_0)$  of the beam is roughly  $\vartheta \approx 1/130$  so that second-order effects ( $O[\vartheta^2]$ ) are negligible as compared with the first-order effects given by Eqs. (4) and (5). Second-order effects may become relevant, for example, in the proximity of the Brewster angle (typically within  $10^{-4}$  rad) in air-to-glass reflection processes. We do have full second-order versions of Eqs. (4) and (5), but they are so cumbersome that there is no room for them in the format of a Letter. They will appear in a full research paper that is in preparation.
20. Note that in [11] the authors use a lens L2 with focal length  $z_{\text{eff}}$  to collimate the beam so that  $\langle y_r \rangle$  remains constant after passing L2.